Supporting Information

Controlled Evaporation-Induced Phase Separation of Droplets Containing Nanogels and Salt Molecules

Yuandu Hu*

*Departments of Materials Science and Engineering, Department of Physics, School of Physical Science and Engineering, Beijing Jiaotong University, Beijing, China

Email: huyd@bjtu.edu.cn

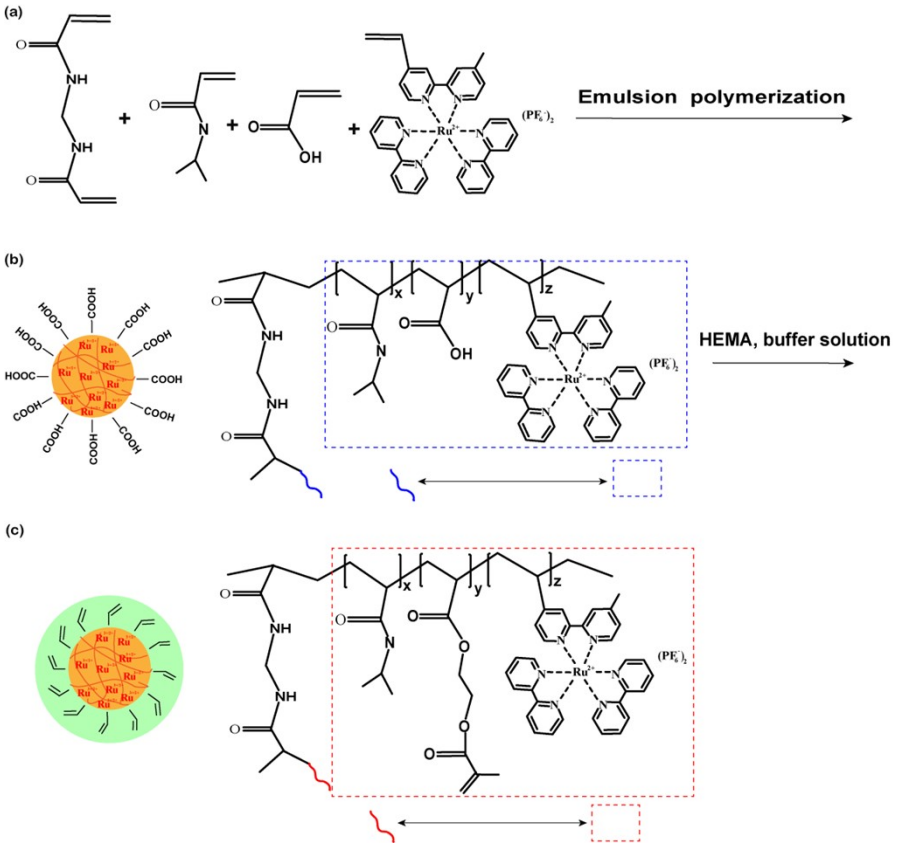

Figure S1. Synthetic routes of pNIPAAm-AAc-Ruthenium gel particles and HEMA modified pNIPAAm-AAc-Ruthenium gel particles.

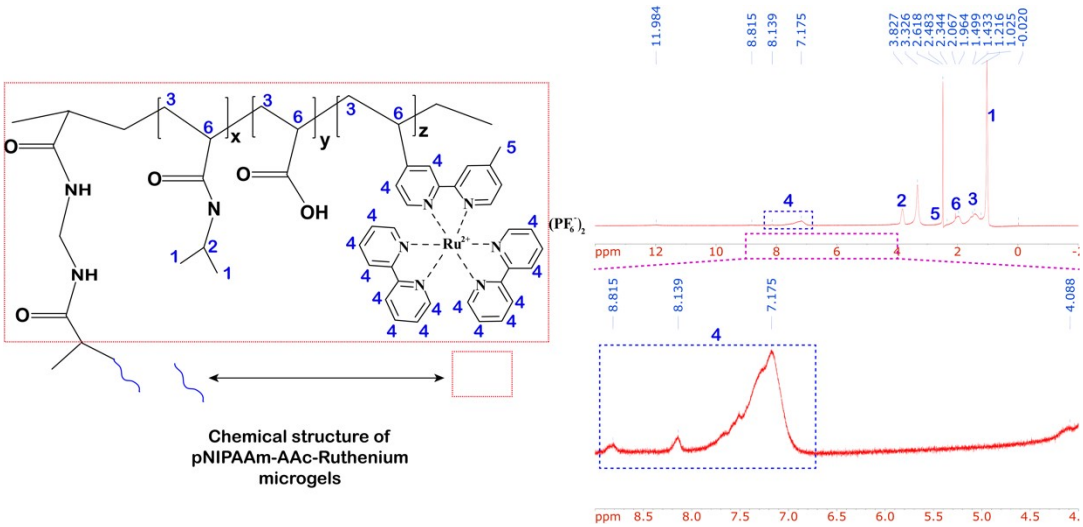

Figure S2. ^{1}H NMR spectrum of the pNIPAAm-AAc-Ruthenium nanogels.

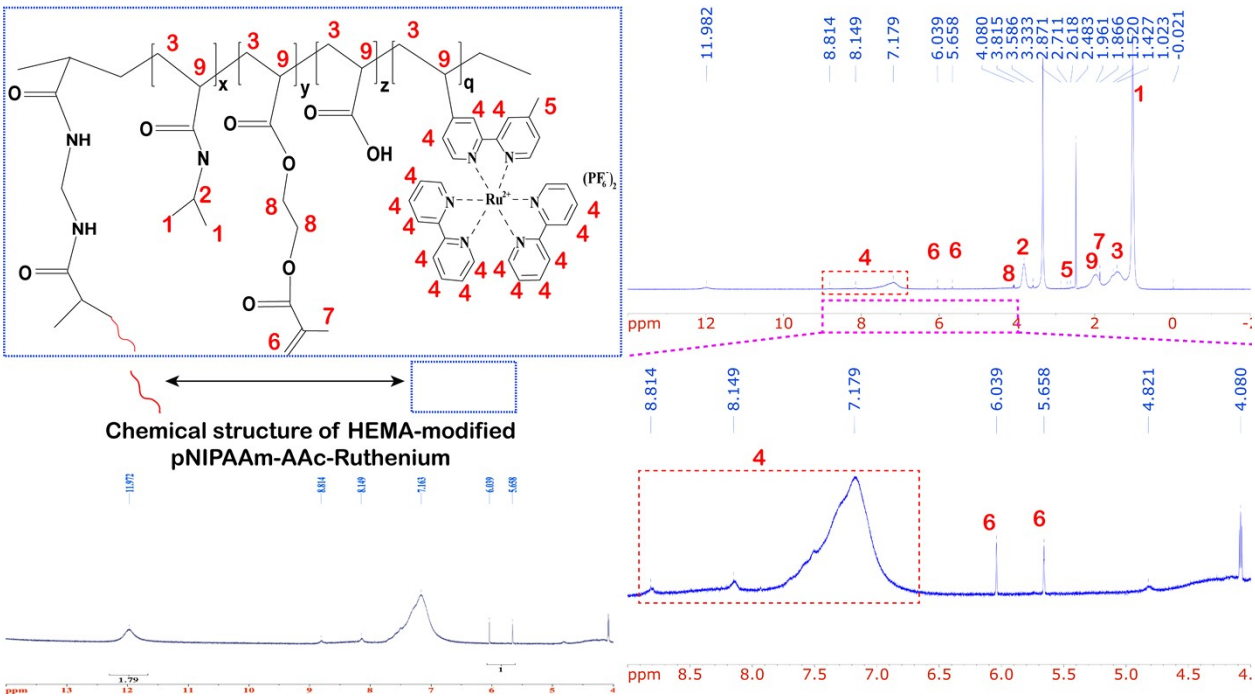

Figure S3. ^{1}H NMR spectrum of the HEMA-modified pNIPAAm-AAc-Ruthenium nanogels.

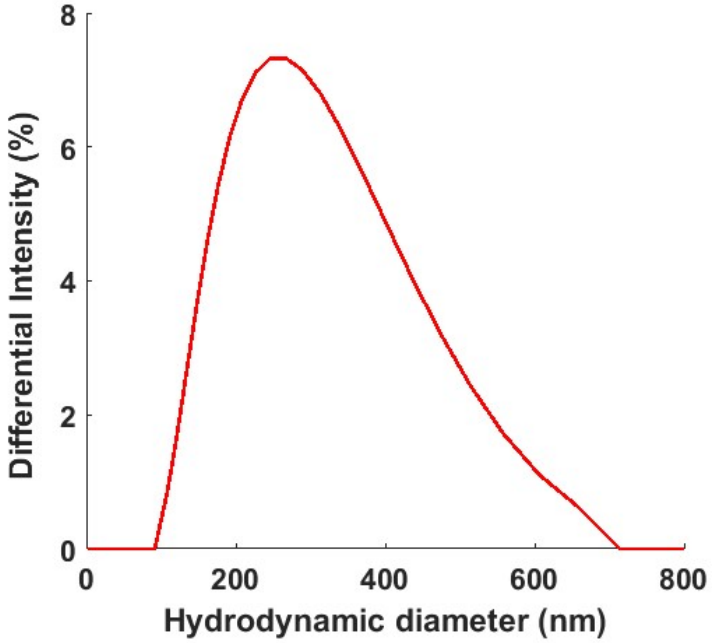

Figure S4. DLS result of the HEMA-modified pNIPAAm-AAc-Ruthenium nanogels.

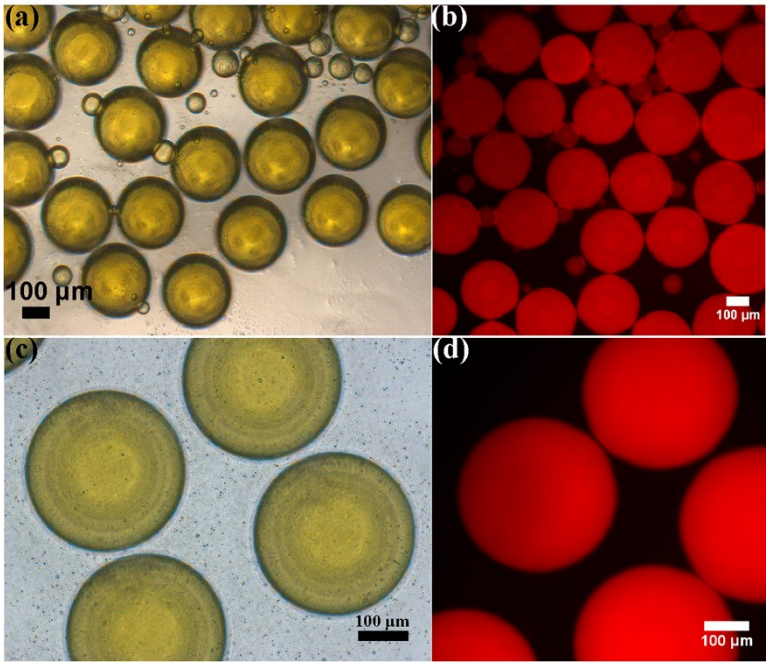

Figure S5. Optical microscopy images of two separate batches (a and c) of droplet samples just produced from microfluidics and collected in two containers, respectively. (c) and (d) are the corresponding fluorescence microscopy images of the two samples. The fluorescence microscopy images indicate that there were no obvious gel particle aggregates at very beginning. At least, there

was no detectable nanogel aggregates caused by electrostatic screening effect when the concentrations of salt molecules were below a certain value, for example, the salt concentrations at this moment was ~ 0.15 M. This phenomenon is consistent with our previous study that there were no microscopic scale gel particle aggregations when the concentration of $NaBrO_3$ was below 0.2 M.[1]

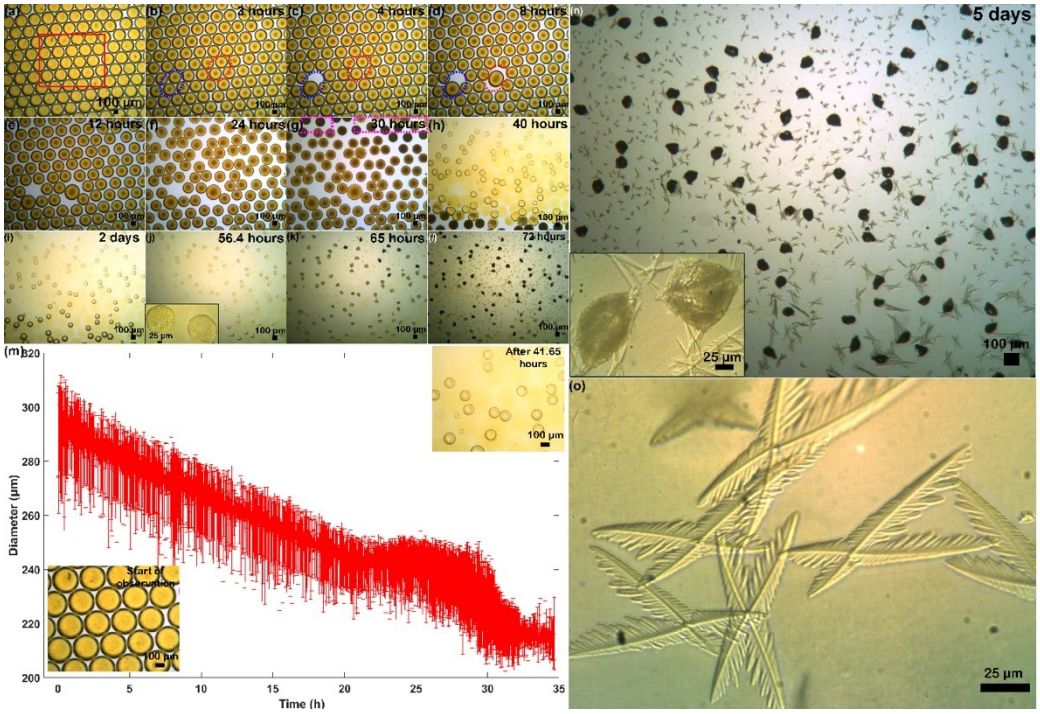

Figure S6. (a)-(f). Optical microscopy images of the evolution of another batch of droplets simply under solvent evaporation. The square in (a) indicates the population of droplets that were statistically measured their sizes and their sizes evolution was plotted in (m). (n). Optical microscopy image of the droplets after 5 days of evolution. The photo indicates droplets were transformed into gel particle-based aggregates and crystal-like structures. (o). Optical microscopy image of the enlarged branched crystal-like structures.

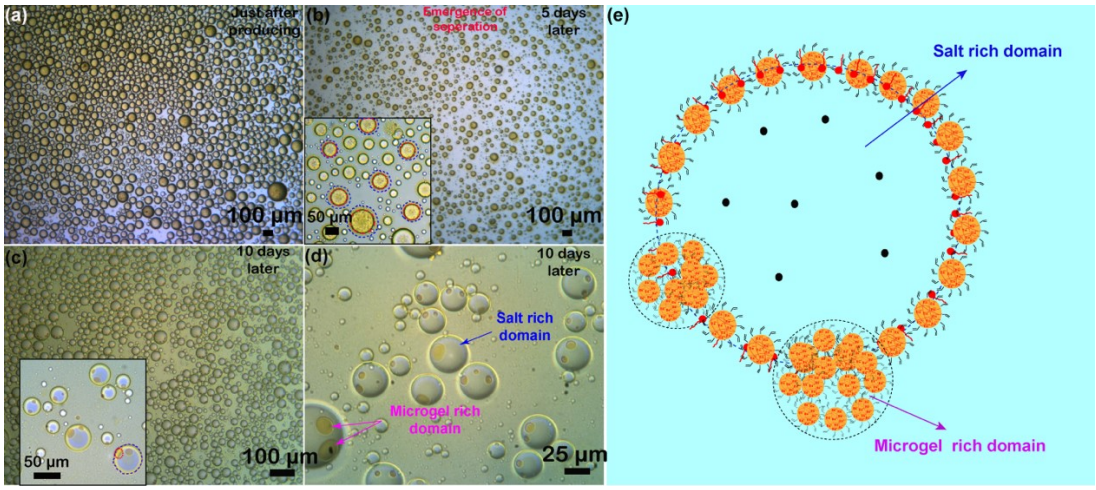

Figure S7. (a) Optical microscopy images of nanogel-containing droplets prepared by hand shaking and with smaller sizes than that of from microfluidics. (b) - (c) The evolution of the droplets at different stages revealed that there was a phase separation process, which induced the initially homogeneous droplets gradually evolved into droplets with buddings. (d) Enlarged microscopy figure of image (c). These budded droplets are composed of two parts: gel particle-rich part and salt-rich part. (e) Illustration figure of the complex droplets in (d).

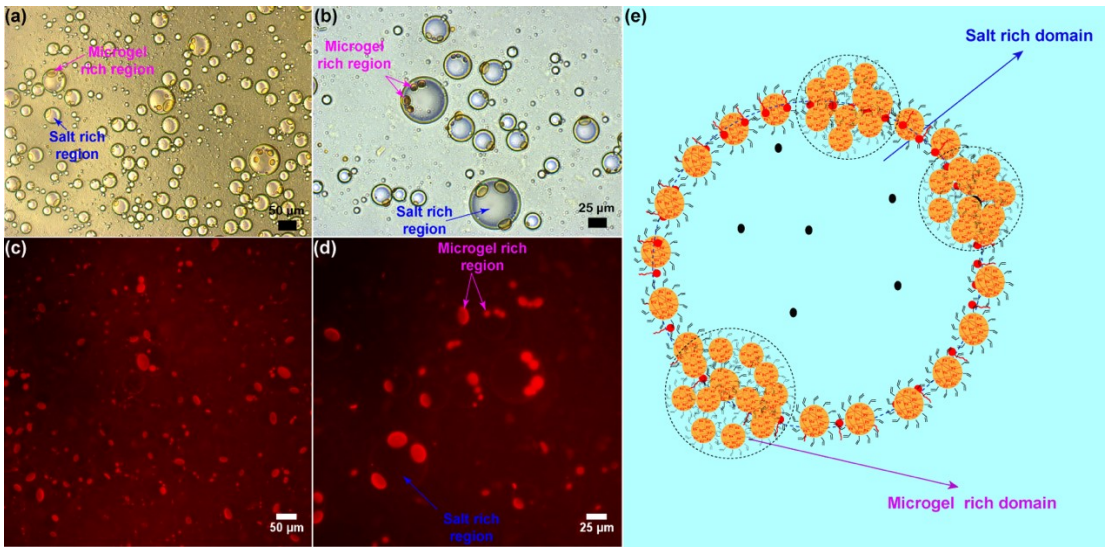

Figure S8. Optical microscopy images of gel particle-containing droplets after 10 days of evolution: (a) - (b) Bright field; (c) - (d) Fluorescent mode. The evolved droplets displayed different fluorescence features, further confirming that the initial homogeneous droplets gradually evolved into droplets composed of gel particle-rich part and salt rich part. (e) Illustration figure of the complex droplets in the left microscopy images (a - d).

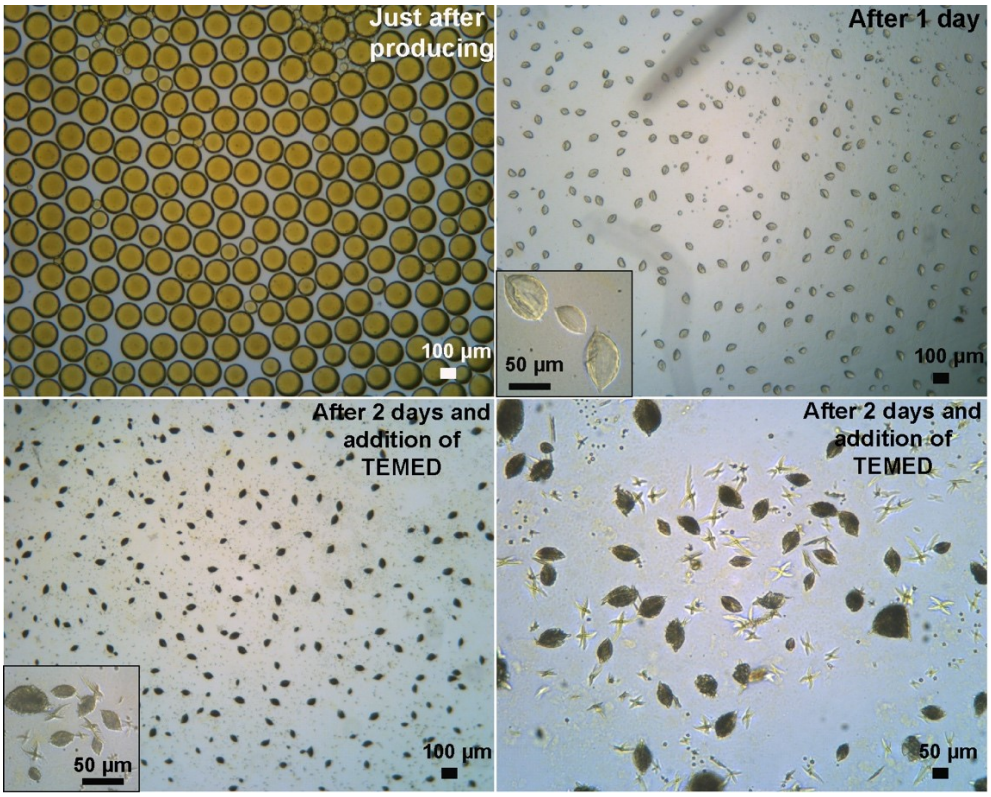

Figure S9. Optical microscopy images show the evolution of nanogel-containing droplets with an average smaller diameter of ~ 150 µm. The droplets eventually evolve into two separate parts: Chinese dumpling-like gel particle-rich aggregates and butterfly-like salt-rich crystal-like structures.

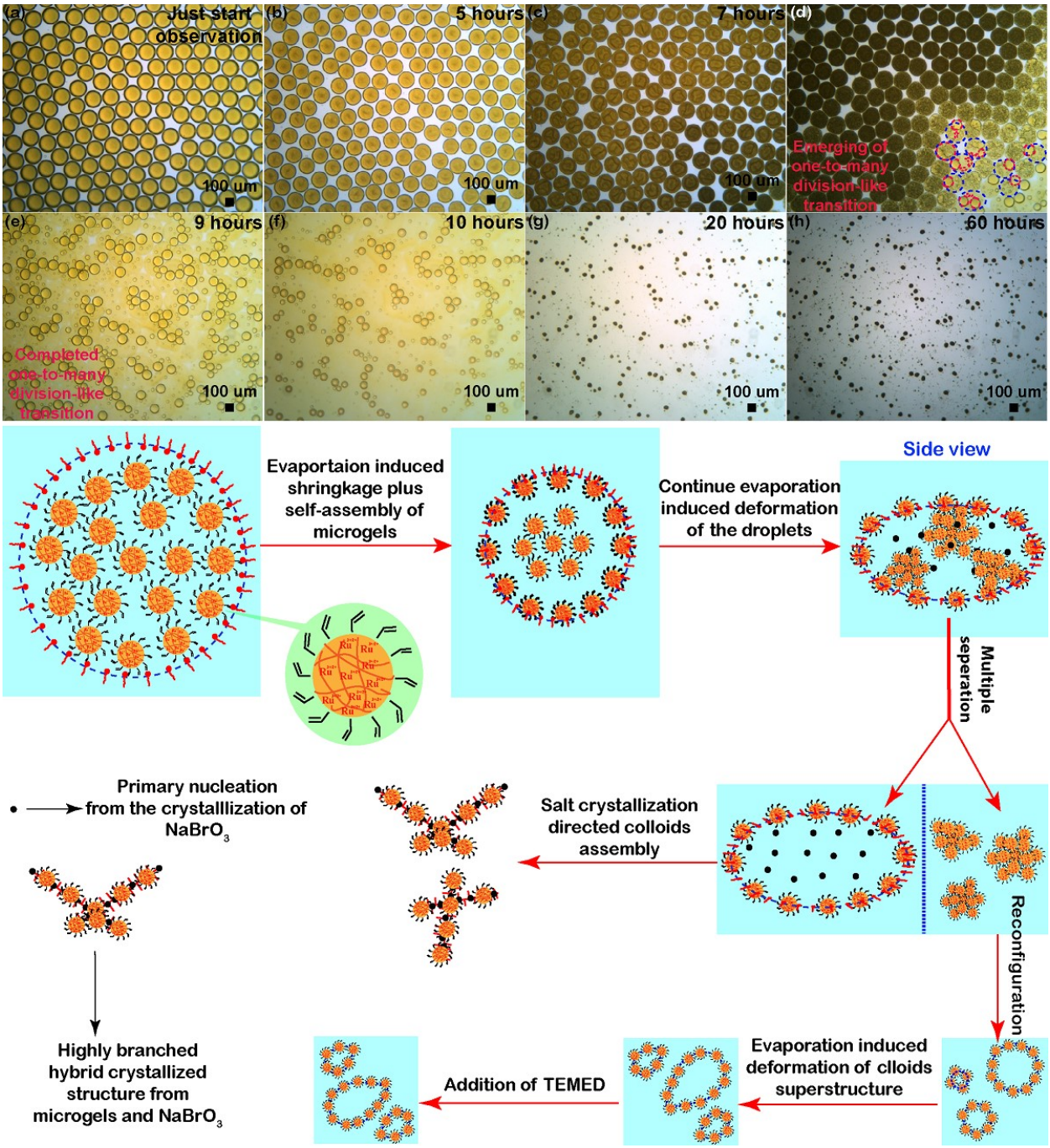

Figure S10. Top: Optical microscopy images of nanogel-containing droplets displaying one-to-many division-like evolution behavior. (a) - (b) Droplet's size decrease process; (b) - (c) Shape change process of the droplets. (d) - (e) Droplets undergo one-to-many division-like transition. (f) Completion of the transition of droplets. (g) - (h) Continued evaporation of solvent in gel particle-containing droplets. Bottom: Carton figure illustrates one-to-many evolution of the gel particle-containing droplet.

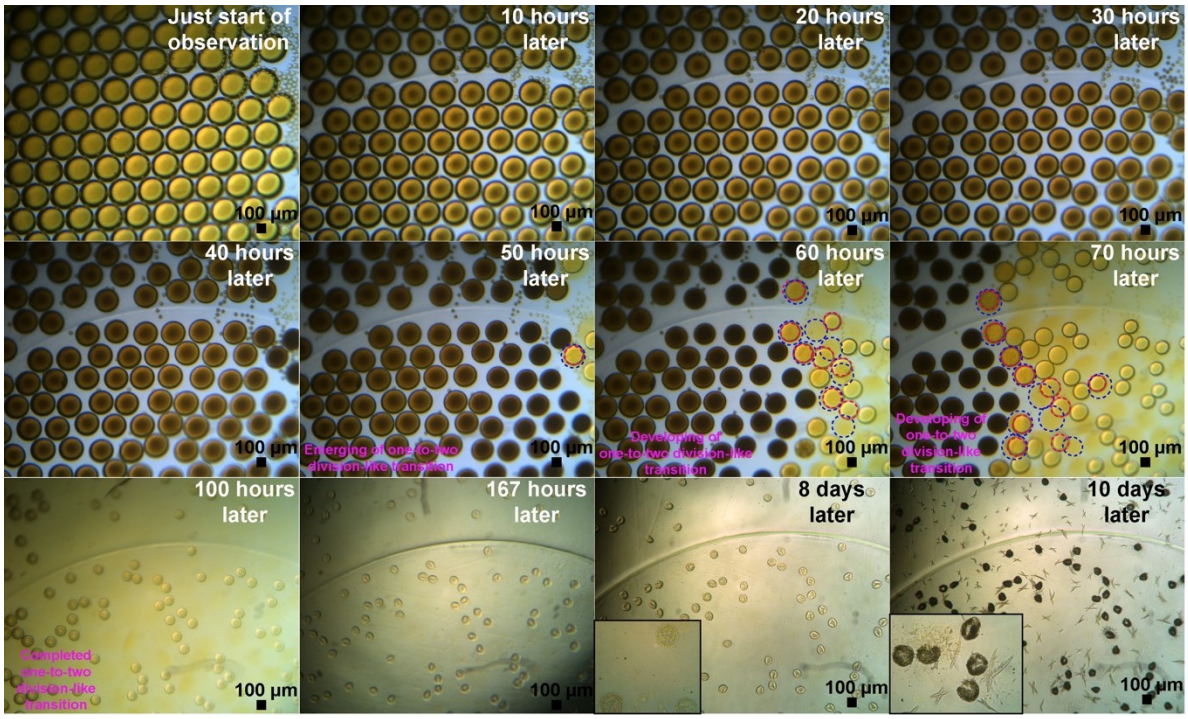

Figure S11. Optical microscopy images show that a population of droplets containing nanogels evolved under a relatively slow solvent evaporation condition. The droplets displayed a one-to-two replication-like feature. Despite the solvent evaporation rate is slower than that of other sets of experiments, the droplets show a similar trend as that of the droplets under higher solvent evaporation rate conditions.

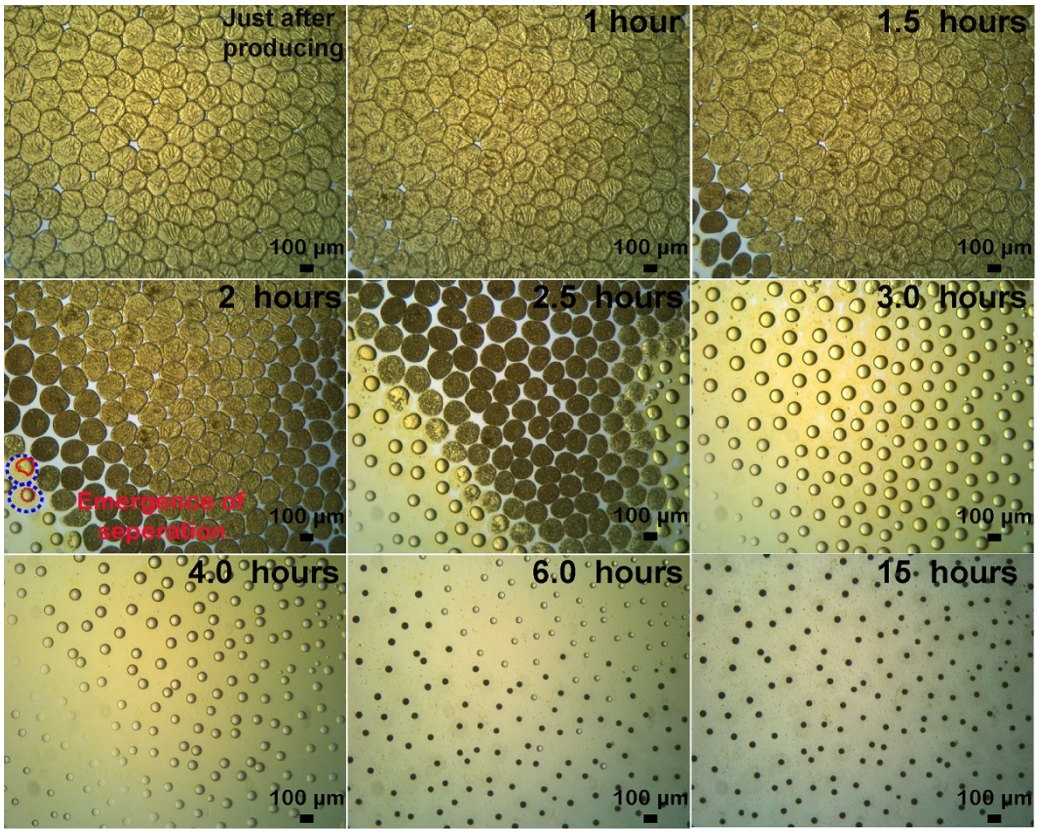

Figure S12. Optical microscopy images show that the evolution of a population of droplets containing nanogels but with deformed shape. Despite the shape of the initial droplets is not spherical and the $NaBrO_3$ concentration is relatively higher, the gel particle-containing droplets still underwent a phase separation in the sample evolution process. Higher concentration of $NaBrO_3$ also advanced the separation process, which took place in a very short period after the droplets were produced. For example, it only takes about 1.5 hours for the droplets to start to undergo the phase separation process under the same evaporation condition.

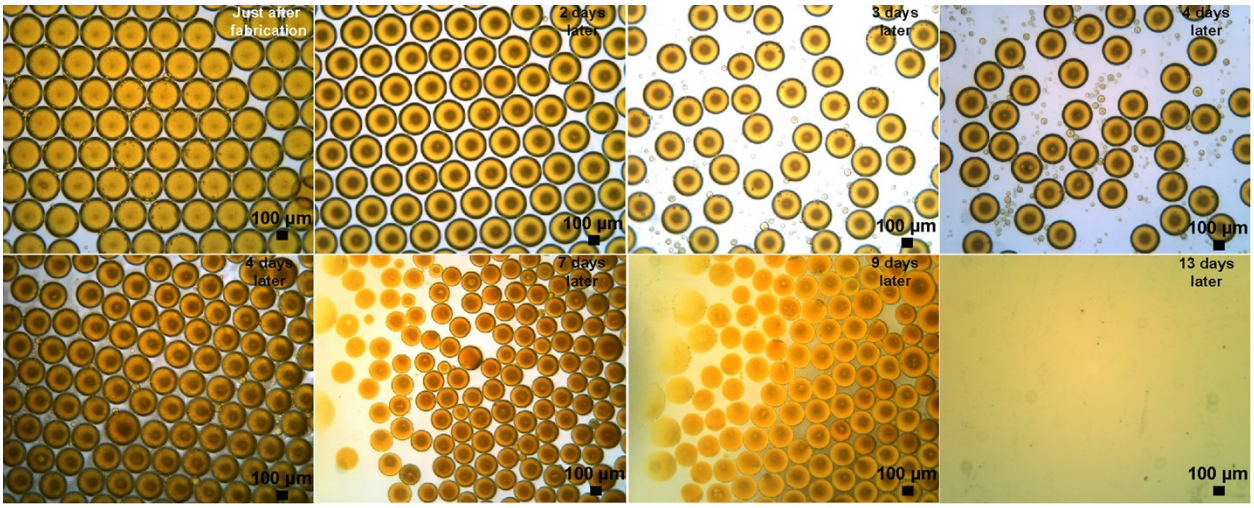

Figure S13. Microscopy images of the evolution of gel particle-containing droplets without addition of $NaBrO_3$ and in a slow evaporation fashion (The droplets transformation process takes places within ~10 days). The evaporation was monitored over a period of 13 days. Unlike the evolution of droplets with nanogels, the evolution of the nanogel-free droplets ends up with almost a blank background (with very small amount of gel particle residues). which is very similar to that of the droplets evolve in a fast evaporation mode. This experiment indicates that it is indispensable for droplets to contain $NaBrO_3$ composition to ensure the occurrence of phase separation process. And the occurrence of phase separation process is independent of the solvent evaporation rate in our observation range.

Supposing the concentrations of $NaBrO_3$ of the droplet's solution at the initial state and at any given point t are C_i and C_t, respectively, while the corresponding diameters of the droplet are d_i and d_t, given the fact of that the total amount of $NaBrO_3$ in each droplet is constant at m before undergoing crystallization, where

$$m = C_i*\Pi*4(d_i/2)^3 = C_t*\Pi*4(d_t/2)^3$$

Therefore, the relationship between these two parameters is:

$$C_t = C_i*(d_i/ d_t)^3$$

Similarly, the time-dependent concentration c_t of gel particles in the droplet is as follows:

$$c_t = c_i*(d_i/ d_t)^3$$

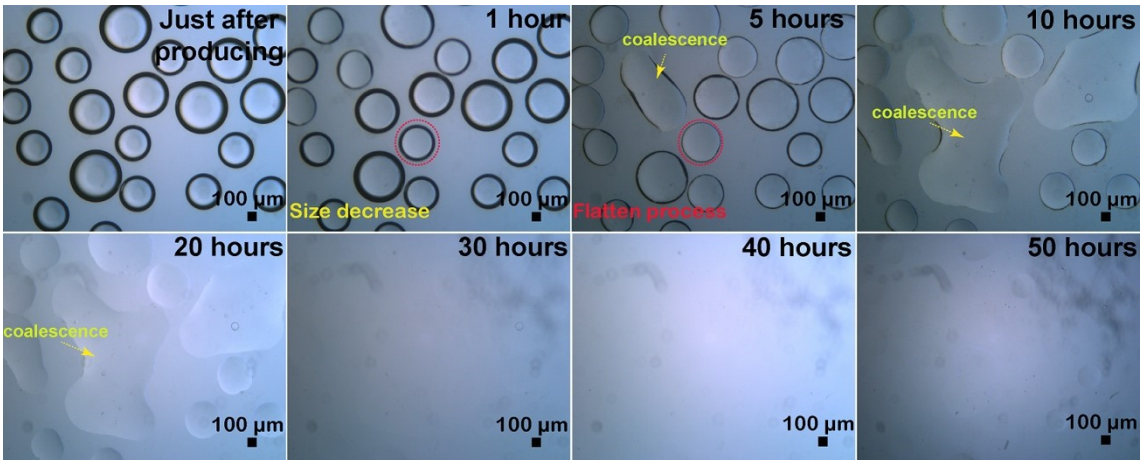

Figure S14. Evolution process of nanogel-free droplets under optical microscopy. The droplets underwent size decrease process and followed with a flatten process but without showing any separation phenomenon as that of the droplets containing nanogels. In addition, the large interfacial tension between the droplets and external Span 80/1-Decanol solution prevents the droplets from keeping stable, which gradually leads to the coalescence of droplets. The absence of showing the phase separation process in this set of experiment indicates that nanogels are critical for the droplets' separation process.

Appendix

Experiment Number	3 wt% gel particle solution	2 M $NaBrO_3$ Solution	1 wt% KPS solution	H_2O	Corresponding to Figures
1	500	50	83	175	Figure 2, S5-S9, S11-S12
2	500	50	83	0	Figure S10
3	500	0	0	0	Figure S3 and Figure S13
4	0	50	83	500	Figure S14

Droplets' compositions in different Figures

Droplets Preparation Method	Microfluidics	Handshaking
Corresponding to Figures	Figure 2-3, Figure S5-6, Figure S9-14	Figure S7-8

Droplets composition in different Figures

The above-mentioned table refers to the droplet composition in the study of the manuscript. The external oil phase in all the experiments was decanol solution of span 80(5 wt%).

Droplets Evaporation Rate	Slow	Slower
Corresponding Figures	Figure 2-3, Figure S6, Figure S9-10, Figure S14	Figure S7-8, Figure S11, Figure S13

Droplet evaporation rates in different Figures

(Note: All the experiments were conducted at slow (sample was loosely covered with a petri dish cover or tightly covered with a petri dish cover.)

References:

[1] Y. Hu, J. Perez-Mercader *Macromol Rapid Commun*. **2017**, *38*, DOI: 10.1002/marc.201600577.